Position-Domain Hatch Filter for Kinematic Differential GPS/GNSS

H. K. Lee, *Member, IEEE*, and C. Rizos

***Abstract*—Motivated by the accuracy benefit of the Hatch gain compared to the Kalman-type gain and the advantage of position-domain filtering compared to range-domain filtering, this paper proposes a position-domain Hatch filter for differential kinematic satellite-based positioning. It is shown that the Hatch gain generates white residual sequence in both the range-domain and the position-domain. An experiment result demonstrates that the proposed position-domain Hatch filter is advantageous in real time kinematic positioning.**

***Index Terms*—Kalman, Hatch, filter, analysis**

I. Introduction

UNLIKE many other positioning sensors, a Global Navigation Satellite System (GNSS) receiver provides diverse measurements. This diversity of measurements offers an opportunity for improvements in both positioning accuracy and fault detection ability. The carrier-smoothed-code filtering proposed by Hatch [1] is a good example of an algorithm that maximally utilizes the information redundancy provided by GNSS to improve positioning accuracy. Compared with other types of filtering for precise differential positioning, carrier-smoothed-code filtering does not require the specification of a dynamic model or the provision of fast-rate aiding sensors for time propagation.

After the introduction of the Hatch filter, several position-domain (PD) filters have also been proposed that exhibit less sensitivity to changes in the visible satellite constellation. The two most representative examples of these are the complementary filter proposed by Hwang and Brown [2] and the phase-connected filter proposed by Bisnath and Langley [3]. The complementary filter utilizes the receiver's current position as the filter states and the phase-connected filter utilizes the current and the previous position as the filter states. Thus, the phase-connected filter requires twice the number of states of the complementary filter. Recently, it was shown that position-domain is more beneficial than range-domain in applying carrier-smoothed -code technique to urban GPS data [4-8].

This study is motivated by a covariance analysis result that compares two representative range-domain (RD) carrier-smoothed-code filters, i.e., the well-known Hatch filter [1] and the RD filter that utilizes Kalman-type gain [7]. Fig. 1 shows the covariance analysis result that illustrates the steady state performance of both RD filters. In the figure, the horizontal axis corresponds to the carrier-to-code noise ratio where representative values for single-frequency, ionosphere-free combination, and wide-lane measurements [2], [9]−[12] are depicted. The vertical axis shows the error reduction ratio where the variance of the smoothed code is divided by that of the raw pseudorange. It can be seen that the Hatch filter shows better performance than the Kalman-type RD filter. In addition, the performance difference grows as the carrier-to-code noise ratio increases. The Kalman-type gain satisfies a certain optimality criteria. As a result, it is also anticipated that the Hatch gain has its own optimality criteria (and other favorable characteristics), that will be proven later.

The other motivation came from the comparison of results from PD and RD filters. As will be seen later, RD filtering is in general more susceptible to information loss than PD filtering if signal lock of a channel is lost, even for a short period [8].

Motivated by these two insights, this paper proposes an efficient kinematic PD filter, that the authors refer to as the PD Hatch filter. The proposed PD Hatch filter enables more accurate position estimation in the presence of signal blockages. This is due to the synergism of both Hatch gain and PD filtering.

To prove the advantages of the PD Hatch filter, this paper is organized as follows. In Section 2, assumptions and the measurement model are introduced. A class of PD and RD filters are summarized. In Section 3, a new interpretations of the RD Hatch filter are provided. Extending the interpretation results of the RD Hatch filter, the PD Hatch filter is derived. In Section 4, an experiment result is presented to demonstrate the benefits of the PD Hatch filter. Finally, a concluding remark will be given.

Manuscript received April 2, 2004. This work was supported the Korea Science and Engineering Foundation.

H. K. Lee was with the Satellite Navigation and Positioning Group, School of Surveying and Spatial Information Systems, University of New South Wales, Australia. He is now with the School of Electronics, Telecommunication and Computer, Hankuk Aviation University, 200-1, Hwajon-dong, Deokyang-gu, Goyang-city, Kyunggi-do, 412-791, Korea (phone: +82-2-300-0131; fax: +82-2-3159-9257; e-mail: hyknlee@ hau.ac.kr).

C. Rizos is with the Satellite Navigation and Positioning Group, School of Surveying and Spatial Information Systems, University of New South Wales, Australia (e-mail: c.rizos@unsw.edu.au).

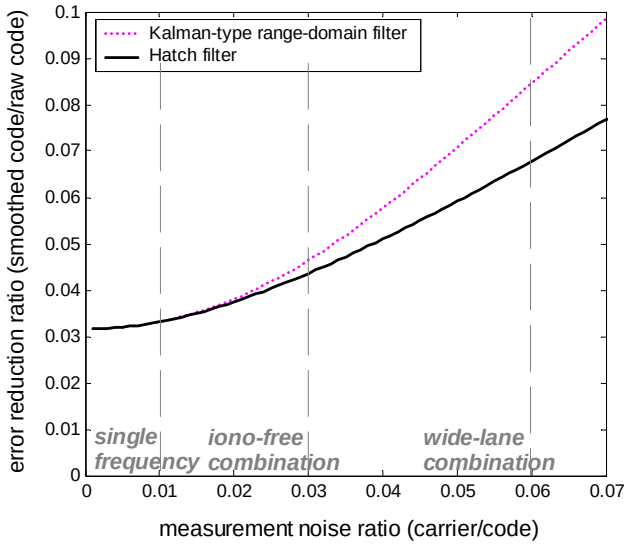

Fig. 1. Comparison of the *a priori* error between the Hatch filter and the stepwise-optimal range-domain filter

II. Summary of Carrier-Smoothed-Code Filters

A. Assumptions and Measurement Model

To extract the complete information transmitted by a GNSS satellite, a receiver's channel typically consists of two signal tracking loops, the Delay Lock Loop (DLL) and the Phase Lock Loop (PLL) [9], [13]– [16]. The DLL is responsible for generating the pseudoranges, while the PLL generates the accumulated carrier phase observables. The pseudoranges and carrier phases measured by a single receiver are contaminated by a variety of error sources, including thermal noise, satellite-oriented error, ionospheric delay, tropospheric delay, cycle slip, and multipath disturbance.

If a user's receiver and a reference receiver are located close by or dual-frequency receivers are used, the common error sources such as the satellite-oriented error, ionospheric delay, and tropospheric delay can be effectively eliminated [9]– [13]. This type of data combination is referred to as *single-differencing*. Cycle slips can be detected by comparing L1 carrier phase with L2 carrier, L1 doppler shift, or estimated velocity and clock bias projected along the line of sight direction. Multipath error can be effectively detected and mitigated by various known methods [6], [14], [15], [17]– [20]. Since this study focuses only on the efficiency of position estimation, the corrected pseudorange $\widetilde{\rho}_{j,k}$ and carrier phase $\widetilde{\phi}_{j,k}$ with respect to the j-th satellite at the k-th epoch (assuming the common-mode errors, cycle slips, and multipath errors have been eliminated) can be modeled as:

$$\widetilde{\rho}_{j,k} = e_{j,k}^T (x_{j,k} - x_{u,k}) + b_{u,k} + v_{j,k}$$
$$\widetilde{\phi}_{j,k} = e_{j,k}^T (x_{j,k} - x_{u,k}) + b_{u,k} + n_{j,k} + \lambda \mathsf{N}_j$$

$$\begin{bmatrix} v_{j,k} \\ v_{j,k+1} \\ v_{j+1,k} \\ n_{j,k} \\ n_{j,k+1} \\ n_{j+1,k} \end{bmatrix} \sim \left(\begin{bmatrix} 0 \\ 0 \\ 0 \\ 0 \\ 0 \\ 0 \end{bmatrix}, \begin{bmatrix} r_\rho & 0 & 0 & 0 & 0 & 0 \\ 0 & r_\rho & 0 & 0 & 0 & 0 \\ 0 & 0 & r_\rho & 0 & 0 & 0 \\ 0 & 0 & 0 & r_\phi & 0 & 0 \\ 0 & 0 & 0 & 0 & r_\phi & 0 \\ 0 & 0 & 0 & 0 & 0 & r_\phi \end{bmatrix} \right) \quad (1)$$

where

$e_{j,k}$: Line of Sight (LOS) vector from the receiver to the j-th satellite at the k-th epoch

$x_{j,k}$: Earth-Centered Earth-Fixed (ECEF) position of the j-th satellite at the k-th epoch

$x_{u,k}$: ECEF receiver position at the k-th epoch

$b_{u,k}$: receiver clock bias at the k-th epoch

N_j : unresolved integer ambiguity

$v_{j,k}$, $n_{j,k}$: noise terms in the code and carrier measurements of the j-th satellite at the k-th epoch

r_ρ, r_ϕ : uniform noise strength values of code and carrier measurements

$\sim (m, P)$: Gaussian distribution of appropriate dimension with the mean m and the covariance P

A typical noise ratio for $\sqrt{r_\phi / r_\rho}$ is of the order of 0.01 if single-frequency receivers are used. It can range, however, to 0.06 if the wide-lane combination of a dual-frequency receiver is used [9]– [13]. Though not considered, it is worth remarking that the carrier-smoothed-code filtering can also be applied to other types of radio-navigation signals, not just to the signals from GNSS satellites. In this case, the noise ratio will vary.

The symbol X_k will be used to denote the true state vector, that is composed of the three-dimensional position sub-vector $x_{u,k}$ and the receiver clock bias $b_{u,k}$:

$$X_k := \begin{bmatrix} x_{u,k} \\ \cdots \\ b_{u,k} \end{bmatrix} \quad (2)$$

Related to the true state vector X_k, the symbols $\overline{X}_k$, $\delta\overline{X}_k$, $\overline{P}_k$, $\hat{X}_k$, $\delta\hat{X}_k$, and $\hat{P}_k$ will be used to represent the *a priori* state estimate, *a priori* estimation error, *a priori* error covariance matrix, *a posteriori* state estimate, *a posteriori* estimation error, and *a posteriori* error covariance matrix at the k-th step for all the filters considered, respectively:

$$\overline{X}_k = \begin{bmatrix} \overline{x}_{u,k} \\ \cdots \\ \overline{b}_{u,k} \end{bmatrix}, \quad \delta\overline{X}_k := \overline{X}_k - X_k = \begin{bmatrix} \delta\overline{x}_{u,k} \\ \cdots \\ \delta\overline{b}_{u,k} \end{bmatrix}, \quad \delta\overline{X}_k \sim (O, \overline{P}_k),$$
$$\hat{X}_k = \begin{bmatrix} \hat{x}_{u,k} \\ \cdots \\ \hat{b}_{u,k} \end{bmatrix}, \quad \delta\hat{X}_k := \hat{X}_k - X_k = \begin{bmatrix} \delta\hat{x}_{u,k} \\ \cdots \\ \delta\hat{b}_{u,k} \end{bmatrix}, \quad \delta\hat{X}_k \sim (O, \hat{P}_k). \quad (3)$$

To denote the true displacement information, the symbol ΔX_k will be used:

$$\Delta X_k := X_{k+1} - X_k = [(\Delta x_{u,k})^T \vdots \Delta b_{u,k}]^T \tag{4}$$

The symbols I and O will be used to notate identity and zero matrices of appropriate dimension. If necessary, their dimensions are explicitly given using subscripts.

B. Position-Domain Filters

The indirect measurement $z_{j,k}$ with respect to $\delta\overline{X}_k$ for measurement update for PD filtering is formed by the following equation:

$$z_{j,k} = \widetilde{\rho}_{j,k} - e_{j,k}^T (x_{j,k} - \overline{x}_{u,k}) - \overline{b}_{u,k} \tag{5}$$

According to (1-5), the indirect measurement z_k^j satisfies

$$z_{j,k} = h_{j,k}\delta\overline{X}_k + v_{k,j},$$
$$h_{j,k} := [e_{j,k}^T \vdots -1]. \tag{6}$$

In PD filters, all the channelwise scalar measurements participate in position estimation concurrently, as they are acquired. Thus, vector notation is more convenient in describing PD filters. The indirect measurement vector Z_k to update the position estimate $\overline{X}_k$ from to $\hat{X}_k$ is written as follows:

$$Z_k = H_k\delta\overline{X}_k + v_k, \quad v_k \sim (O_{J\times 1}, r_\rho I_{J\times J}) \tag{7}$$

where

$$Z_k := \begin{bmatrix} z_{1,k} \\ z_{2,k} \\ \vdots \\ z_{J,k} \end{bmatrix}, \quad H_k := \begin{bmatrix} h_{1,k} \\ h_{2,k} \\ \vdots \\ h_{J,k} \end{bmatrix}, \quad v_k := \begin{bmatrix} v_{1,k} \\ v_{2,k} \\ \vdots \\ v_{J,k} \end{bmatrix}$$

$$h_{j,k} := [e_{j,k}^T \vdots -1]$$

J : number of visible satellites (8)

To derive the exact measurement equation for time-propagation, it is necessary to define the variables $\Delta x_{u,k}$, $\Delta b_{u,k}$, $\Delta x_{j,k}$, and $\Delta e_{j,k}$ as the increments of the user position, user receiver clock bias, the j-th satellite's position, and the LOS vector from the k-th step to the $(k+1)$-th step, respectively:

$$\Delta x_{u,k} := x_{u,k+1} - x_{u,k},\ \Delta b_{u,k} := b_{u,k+1} - b_{u,k}$$
$$\Delta x_{j,k} := x_{j,k+1} - x_{j,k},\ \Delta e_{j,k} := e_{j,k+1} - e_{j,k} \tag{9}$$

Then, according to (1) and (9), the incremental carrier phase $(\widetilde{\phi}_{j,k+1} - \widetilde{\phi}_{j,k})$ satisfies the condition:

$$\widetilde{\phi}_{j,k+1} - \widetilde{\phi}_{j,k} = -(e_{j,k} + \Delta e_{j,k})^T \Delta x_{u,k} + n_{j,k+1} - n_{j,k} + \Delta b_{u,k} + e_{j,k}^T \Delta x_{j,k} + \Delta e_{j,k}^T (x_{j,k+1} - x_{u,k}) \tag{10}$$

If one forms the indirect measurement $\omega_{j,k+1}$ for time-propagation as:

$$\omega_{j,k+1} := e_{j,k}^T \Delta x_{j,k} + \Delta e_{j,k}^T (x_{j,k+1} - \hat{x}_{u,k}) - (\widetilde{\phi}_{j,k+1} - \widetilde{\phi}_{j,k}) \tag{11}$$

$\omega_{j,k+1}$ satisfies the following relationship according to (3), (6), and (9)$-$(11):

$$\omega_{j,k+1} = h_{j,k+1}\Delta X_k + w_{j,k+1},$$
$$\Delta X_k = [(\Delta x_{u,k})^T \vdots \Delta b_{u,k}]^T, \tag{12}$$

where

$$w_{j,k+1} := -\Delta e_{j,k}^T \delta\hat{x}_{u,k} - n_{j,k+1} + n_{j,k} \tag{13}$$

Stacking $\omega_{j,k+1}$ for all the satellites into a vector Ω_{k+1} yields the following linear equation to propagate $\hat{X}_k$ in time to $\overline{X}_{k+1}$:

$$\Omega_{k+1} = H_{k+1}\Delta X_k + W_{k+1}$$
$$W_{k+1} = -\Delta H_k \delta\hat{X}_k - n_{k+1} + n_k,\ \ n_k \sim (O_{J\times 1}, r_\Phi I_{J\times J}) \tag{14}$$

where

$$\Omega_{k+1} := \begin{bmatrix} \omega_{1,k+1} \\ \omega_{2,k+1} \\ \vdots \\ \omega_{J,k+1} \end{bmatrix}, \ W_{k+1} := \begin{bmatrix} w_{1,k+1} \\ w_{2,k+1} \\ \vdots \\ w_{J,k+1} \end{bmatrix}, \ n_k := \begin{bmatrix} n_{1,k} \\ n_{2,k} \\ \vdots \\ n_{J,k} \end{bmatrix}$$

$$\Delta H_k := H_{k+1} - H_k \tag{15}$$

Based on the two types of vector measurements Z_k and Ω_{k+1}, the PD filters with consistent error covariance information are implemented in a recursive way using the following algorithm.

Initialization:

$$\hat{X}_{k0} = E[X_{k0} \mid \widetilde{\rho}_{k0}]$$
$$\hat{P}_{k0} = r_\rho [H_{k0}^T H_{k0}]^{-1} \tag{16}$$

Time-Propagation:

$$\overline{X}_{k+1} = \hat{X}_k + U_{k+1}\Omega_{k+1}$$
$$\delta\overline{X}_{k+1} = U_{k+1}[H_k\delta\hat{X}_k - (n_{k+1} - n_k)]$$
$$\overline{P}_{k+1} = U_{k+1}\left\{ \begin{matrix} H_k\hat{P}_k H_k^T \\ + r_\Phi \begin{bmatrix} 2I_{J\times J} - H_k(I_{4\times 4} - K_k H_k)U_k \\ -(U_k)^T (I_{4\times 4} - K_k H_k)^T (H_k)^T \end{bmatrix} \end{matrix} \right\} (U_{k+1})^T$$
$$U_k = [(H_k)^T (Q_k)^{-1} H_k]^{-1} (H_k)^T (Q_k)^{-1}$$
$$Q_k \text{ : weighting matrix for time propagation} \tag{17}$$

Measurement Update:

$$\hat{X}_k = \overline{X}_k - K_k Z_k$$
$$\delta\hat{X}_k = (I_{4\times 4} - K_k H_k)\delta\overline{X}_k - K_k v_k$$
$$\hat{P}_k = (I_{4\times 4} - K_k H_k)\overline{P}_k (I_{4\times 4} - K_k H_k)^T + r_\rho K_k (K_k)^T$$
$$K_k \text{ : weighting matrix for measurement update} \tag{18}$$

As can be seen in the algorithm, two gain parameters Q_k and

K_k affect the efficiency of estimation. Selecting Q_k, K_k, and the carrier noise strength r_ϕ as:

i) $Q_k = cI$, $K_k = \overline{P}_k H_k^T (H_k \overline{P} H_k^T + r_\rho I)^{-1}$, $r_\phi = 0$ (19)

ii) $Q_k = cI$, $K_k = \overline{P}_k H_k^T (H_k \overline{P} H_k^T + r_\rho I)^{-1}$, $r_\phi = E\left[(n_k)^2\right]$ (20)

iii) $Q_k := E\left[W_k W_k^T\right]$, $K_k = \overline{P}_k H_k^T (H_k \overline{P} H_k^T + r_\rho I)^{-1}$, $r_\phi = E\left[(n_k)^2\right]$ (21)

where the symbol c denotes an arbitrary scale factor, several filters are generated. (19), (20), and (21) result in a modification of the complementary filter [2],[11], the stepwise-unbiased PD filter, and the stepwise-optimal PD filter [7], respectively. If the product $\Delta H_k \delta\hat{X}_k$ of the LOS change and the estimation error between subsequent epochs is small compared to carrier measurement noise $(n_k - n_{k+1})$, the weighting matrix Q_k described by (14) and (21) almost equals a scaled identity matrix. Due to the utilization of $Q_k = cI$, the time-propagation of the stepwise-unbiased PD filter characterized by (20) is further simplified from (17) to [7]:

$$\overline{P}_{k+1} = U_{k+1} \begin{bmatrix} \left(1 + \dfrac{2r_\Phi}{r_\rho}\right) H_k \hat{P}_k H_k^T \\ -2r_\Phi H_k (H_k^T H_k)^{-1} H_k^T + 2r_\Phi I \end{bmatrix} (U_{k+1})^T \quad (22)$$

It is shown in [7] that (20) of the stepwise-unbiased PD filter is more attractive than (19) and (21) since it maintains consistent error covariance matrix, keeps good positioning accuracy, and is computationally efficient. For later analyses, the *a priori* error covariance recursion of the stepwise-unbiased PD filter is obtained as follows, combining (18) and (22):

$$\overline{P}_{k+1} = U_{k+1} \begin{bmatrix} \left(1 + \dfrac{2r_\Phi}{r_\rho}\right) H_k \left(\overline{P}_k^{-1} + \dfrac{1}{r_\rho} H_k^T H_k\right)^{-1} H_k^T \\ -2r_\Phi H_k (H_k^T H_k)^{-1} H_k^T + 2r_\Phi I \end{bmatrix} (U_{k+1})^T \quad (23)$$

From now on, the stepwise-unbiased PD filter is described as the PD Kalman-type filter for notational convenience.

C. Range-Domain Filters

RD filters generate two range estimates: a compressed pseudorange $\hat{\rho}_{j,k}$ and a projected pseudorange. The compressed pseudorange $\hat{\rho}_{j,k}$ is the *a posteriori* range estimate that is based on all the code and carrier measurements $\{\widetilde{\rho}_{j,i}\}_{i=0,1,2,\cdots,k}$ and $\{\phi_{j,i}\}_{i=0,1,2,\cdots,k}$ of the j-th satellite at the k-th epoch after the initialization of the filter. The projected pseudorange $\overline{\rho}_{j,k}$ is the *a priori* range estimate before the new pseudorange measurement $\widetilde{\rho}_{j,k}$ at the current k–th step is accommodated. The scalar estimation error and error covariance values of $\hat{\rho}_{j,k}$ and $\overline{\rho}_{j,k}$ are denoted by $\hat{v}_{j,k}$, $\hat{R}_{j,k}$, $\overline{v}_{j,k}$ and $\overline{R}_{j,k}$, respectively. The RD filter of the j-th satellite's channel is summarized as follows [7],[8].

Initialization:

$$\alpha_{j,k0} = 0,\ \beta_{j,k0} = 1,\ \hat{\rho}_{j,k0} = \widetilde{\rho}_{j,k0},\ \hat{R}_{j,k0} = r_\rho$$
$$k_0: \text{filter initialization time index } (k > k_0) \quad (24)$$

Time-Propagation: (14c)

$$\overline{\rho}_{j,k+1} := \hat{\rho}_{j,k} + (\widetilde{\phi}_{j,k+1} - \widetilde{\phi}_{j,k})$$
$$\overline{v}_{j,k+1} := \hat{v}_{j,k} + (\widetilde{\phi}_{j,k+1} - \widetilde{\phi}_{j,k})$$
$$\overline{R}_{j,k+1} = \hat{R}_{j,k} + 2\beta_{j,k} r_\Phi \quad (25)$$

Measurement Update:

$$\hat{\rho}_{j,k} = (1 - \beta_{j,k})\overline{\rho}_{j,k} + \beta_{j,k}\widetilde{\rho}_{j,k}$$
$$\hat{v}_{j,k} = (1 - \beta_{j,k})\overline{v}_{j,k} + \beta_{j,k} v_{j,k} = \overline{v}_{j,k} - \beta_{j,k}(\overline{v}_{j,k} - v_{j,k})$$
$$\hat{R}_{j,k} = (1 - \beta_{j,k})^2 \overline{R}_{j,k} + (\beta_{j,k})^2 r_\rho$$
$$\beta_{j,k}: \text{arbitrary gain for the } j\text{-th channel at the } k\text{-epoch} \quad (26)$$

Compared to PD filters, RD filters need no permanent storage for position estimates. Instead, the position estimates are generated at each time by treating the outputs of multiple RD filters $\{\hat{\rho}_{j,k}\}_{j=1,2,\cdots,J}$ or $\{\overline{\rho}_{j,k}\}_{j=1,2,\cdots,J}$ in the same manner as applied to the raw pseudoranges $\{\widetilde{\rho}_{j,k}\}_{j=1,2,\cdots,J}$ for each k.

$$\overline{X}_k^r = E[X_k \mid \overline{\rho}_k], \qquad \hat{X}_k^r = E[X_k \mid \hat{\rho}_k] \quad (27)$$

Since the equivalent pseudoranges of different channels are assumed to be not correlated to each other, the following error covariance matrix $\overline{P}_k^r$ and $\hat{P}_k^r$ of the range-domain filters can represent the accuracy of the resultant position estimate based on RD filters:

$$\overline{P}_k^r = \left[H_k^T (\overline{\Sigma}_k^r)^{-1} H_k\right]^{-1}, \quad \hat{P}_k^r = \left[H_k^T (\hat{\Sigma}_k^r)^{-1} H_k\right]^{-1} \quad (28)$$

In (28), the superscript r denotes range-domain filtering. The error covariance matrices $\overline{\Sigma}_k^r$ and $\hat{\Sigma}_k^r$ are constructed at each time step by utilizing the scalar error covariance values of all the channelwise RD filters:

$$\overline{\Sigma}_k^r := \begin{bmatrix} \overline{R}_{1,k} & 0 & \cdots & 0 \\ 0 & \overline{R}_{2,k} & \cdots & 0 \\ \vdots & \vdots & \ddots & \vdots \\ 0 & 0 & \cdots & \overline{R}_{J,k} \end{bmatrix}, \ \hat{\Sigma}_k^r := \begin{bmatrix} \hat{R}_{1,k} & 0 & \cdots & 0 \\ 0 & \hat{R}_{2,k} & \cdots & 0 \\ \vdots & \vdots & \ddots & \vdots \\ 0 & 0 & \cdots & \hat{R}_{J,k} \end{bmatrix} \quad (29)$$

RD filtering has a disadvantage in that the total information of a channel is lost if the signal lock to the satellite is lost, even for a short period. For that reason, the dimensions of the matrices H_k, $\overline{\Sigma}_k^r$ and $\hat{\Sigma}_k^r$ shown in (29) are reduced by one when a satellite outage occurs.

As shown in the RD filter algorithm, only the scalar gain

parameter $\beta_{j,k}$ affects the efficiency of RD filtering. Depending on the different formulae for $\beta_{j,k}$ shown below, the two most representative RD filters, i.e. the Hatch filter [1] and the stepwise-optimal RD filter [7] are generated:

$$\beta_{j,k} = 1/k \tag{30}$$

$$\beta_{j,k} = \overline{R}_{j,k} /(\overline{R}_{j,k} + r_\rho) \tag{31}$$

By the information sharing principle [21], the measurement update of the stepwise-optimal RD filter can also be represented by (32), instead of (26):

$$\hat{R}_{j,k} = \left(\overline{R}_{j,k}^{-1} + r_\rho^{-1}\right)^{-1} \tag{32}$$

For later analysis, the *a priori* covariance recursion of the stepwise-optimal RD filter is obtained as follows by combining (25), (31), and (32):

$$\overline{R}_{j,k+1} = \left(1 + \frac{2r_\phi}{r_\rho}\right)\left(\overline{R}_{j,k}^{-1} + r_\rho^{-1}\right)^{-1} \tag{33}$$

To contrast the characteristics from the RD Hatch filter, the RD stepwise-optimal filter is described as the RD Kalman-type filter type for notational convenience.

III. POSITION-DOMAIN HATCH FILTER

A. New Interpretation of Range-Domain Hatch filter

Assume that the code and carrier sequences up to the k-th time step are given as $\{\widetilde{\rho}_{j,l}\}$ and $\{\widetilde{\phi}_{j,l}\}$ where $l = 1,2,\cdots,k$. The RD Hatch filter assigns equal weighting of $1/k$ to all the measurements $\{\widetilde{\rho}_{j,l} + (\widetilde{\phi}_{j,k} - \widetilde{\phi}_{j,l})\}$ where $l = 1,2,\cdots,k$. The smoothed pseudorange estimate $\hat{\rho}_{j,k}$ satisfies the following relationship:

$$\hat{\rho}_{j,k} = \frac{1}{k}\sum_{l=1}^{k}\left[\widetilde{\rho}_{j,l} + (\widetilde{\phi}_{j,k} - \widetilde{\phi}_{j,l})\right] \tag{34}$$

Considering all the measurement noise terms, $\hat{\rho}_{j,k}$ can be decomposed as follows:

$$\hat{\rho}_{j,k} = \rho_{j,k} + \hat{v}_{j,k},$$
$$\hat{v}_{j,k} = \frac{1}{k}\sum_{l=1}^{k} v_{j,l} + \frac{1}{k}\sum_{l=1}^{k-1} n_{j,l} + \frac{k-1}{k} n_{j,k}. \tag{35}$$

Due to the independence of the noise terms in (1), the error covariance of the RD Hatch filter satisfies the following relation:

$$\hat{R}_{j,k} := \frac{1}{k} r_\rho + \frac{k-1}{k} r_\phi \tag{36}$$

Substituting (30) and (36) to (25) yields:

$$\overline{R}_{j,k} = \frac{r_\rho + k r_\phi}{k-1} \tag{37}$$

Utilizing (30) and (37), one obtains a new form of RD Hatch gain:

$$\begin{aligned}\beta_{j,k} &= \left(\overline{R}_{j,k} - r_\phi\right)\left(\overline{R}_{j,k} + r_\rho\right)^{-1} \\ &= \left(\overline{R}_{j,k} - r_\phi\right)\left[(\overline{R}_{j,k} - r_\phi) + (r_\phi + r_\rho)\right]^{-1} \\ &= \left[\hat{R}_{j,k-1} + (2\beta_{j,k-1} - 1) r_\phi\right] \\ &\quad \cdot \left\{\left[\hat{R}_{j,k-1} + (2\beta_{j,k-1} - 1) r_\phi\right] + (r_\phi + r_\rho)\right\}^{-1}\end{aligned} \tag{38}$$

By interpreting the gain formula for $\beta_{j,k}$ between the new pseudorange $\widetilde{\rho}_{j,k}$ and the projected pseudorange $\hat{\rho}_{j,k-1} + (\widetilde{\phi}_{j,k} - \widetilde{\phi}_{j,k-1})$, it can be seen that $\beta_{j,k}$ is identical to the optimal gain that combines two projected pseudoranges $\hat{\rho}_{j,k-1} + (\phi_{j,k-\varepsilon} - \widetilde{\phi}_{j,k-1})$ and $\widetilde{\rho}_{j,k} + (\phi_{j,k-\varepsilon} - \widetilde{\phi}_{j,k})$, as shown in Fig. 2, where $\phi_{j,k-\varepsilon}$ stands for a conceptual error-free carrier phase measurement.

To explain the advantages of the RD Hatch filter, the following Theorem 1 summarizes that the RD Hatch filter is a generator of a white residual sequence. Generation of white residual sequence implies that the RD Hatch filter extracts all the useful information that is orthogonal to the noise subspace.

Theorem 1: *White residual generation by RD Hatch filter*

If the noise terms of the corrected measurements satisfy (1), the RD Hatch filter represented by (24)─(26) and (30) generates a white residual sequence. □

B. Derivation of Position-Domain Hatch Filter

In the previous subsection, a new interpretation of the RD Hatch filter was given. The new interpretation showed that the Hatch gain, though its original form is not explicitly related to error statistics as shown in (30), has also a physical meaning from the stochastic point of view, as shown in (38) and Fig. 2. By Theorem 1, it was shown that the Hatch gain extracts all the useful information that is orthogonal to the noise subspace in range-domain.

Based on the new interpretation in the previous subsection, this subsection derives a new PD filter, i.e. the PD Hatch filter. Adopting the simple and efficient weighting $Q_k = I$, as in the case of the PD Kalman-type filtering, the time-propagation of the state estimate $\hat{X}_{k-1}$ at the $(k-1)$-th epoch and the newly arriving measurements $\widetilde{\rho}_k$ of the k-th epoch depicted in Fig. 3 are summarized as follows:

$$\begin{aligned}\overline{X}_{k-\varepsilon} &= \hat{X}_{k-1} + \overline{\Delta X}(\phi_{k-\varepsilon}, \widetilde{\phi}_{k-1}) \\ \overline{\rho}_{k-\varepsilon} &= \widetilde{\rho}_k + \overline{\Delta X}(\phi_{k-\varepsilon}, \widetilde{\phi}_k)\end{aligned} \tag{39}$$

where

$$\begin{aligned}\overline{\Delta X}(\phi_{k-\varepsilon}, \widetilde{\phi}_{k-1}) &:= U_{k-\varepsilon}[\phi_{k-\varepsilon} - \widetilde{\phi}_{k-1} - \Delta H_{k-1}^{k-\varepsilon} X_{k-1}] \\ \overline{\Delta X}(\phi_{k-\varepsilon}, \widetilde{\phi}_k) &:= U_{k-\varepsilon}[\phi_{k-\varepsilon} - \widetilde{\phi}_k - \Delta H_k^{k-\varepsilon} X_k] \\ \Delta H_i^j &:= H_j - H_i\end{aligned} \tag{40}$$

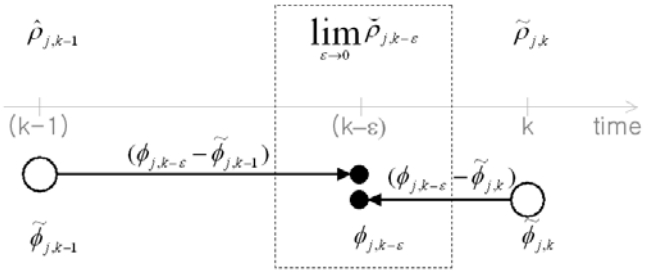

Fig. 2. Projection of compressed pseudorange and raw pseudorange measurement to derive scalar range-domain Hatch gain

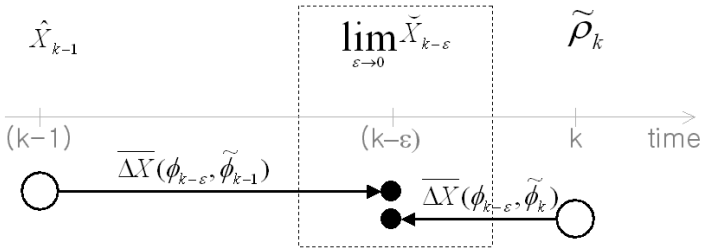

Fig. 3. Projection of state estimate and pseudorange vector to derive vector position-domain Hatch gain

The estimation error $\delta\overline{X}_{k-\varepsilon}$ of the *a priori* state estimate $\overline{X}_{k-\varepsilon}$ in (39) satisfies the following equations.

$$\delta\overline{X}_{k-\varepsilon} = U_{k-\varepsilon}(H_{k-1}\delta\hat{X}_{k-1} + n_{k-1})$$
$$\begin{bmatrix}\delta\hat{X}_{k-1}\\ n_{k-1}\end{bmatrix} \sim \left(O, \begin{bmatrix}\hat{P}_{k-1} & -(I-K_{k-1})U_{k-1}\\ -U_{k-1}^T(I-K_{k-1})^T & r_\phi I\end{bmatrix}\right) \tag{41}$$

By (41), it can be seen that $\delta\overline{X}_{k-\varepsilon}$ satisfies the following Gaussian distribution.

$$\delta\overline{X}_{k-\varepsilon} \sim (O, M_{k-\varepsilon})$$
$$M_{k-\varepsilon} = U_{k-\varepsilon}H_{k-1}P_{k-1}H_{k-1}^T U_{k-\varepsilon}^T + r_\phi U_{k-\varepsilon}\begin{bmatrix}I-H_{k-1}(I-K_{k-1}H_{k-1})U_{k-1}\\ -U_{k-1}^T(I-K_{k-1k-1})^T H_{k-1}^T\end{bmatrix}(U_{k-\varepsilon})^T \tag{42}$$

Applying the procedure that is similar to (5)─(8), the indirect measurement $Z_{k-\varepsilon}$ is obtained from (39)─(41) as follows.

$$Z_{k-\varepsilon} = H_k\delta\overline{X}_{k-\varepsilon} - H_k U_k n_k + v_k \tag{43}$$

Finally, an improved estimate $\breve{X}_{k-\varepsilon}$ can be obtained if one combines $\overline{X}_{k-\varepsilon}$ and $Z_{k-\varepsilon}$ as follows:

$$\breve{X}_{k-\varepsilon} = \overline{X}_{k-\varepsilon} - K_{k-\varepsilon}Z_{k-\varepsilon} \tag{44}$$

As a result of the combination, the estimation error becomes:

$$\delta\breve{X}_{k-\varepsilon} = \delta\overline{X}_{k-\varepsilon} - K_{k-\varepsilon}Z_{k-\varepsilon} \tag{45}$$

Utilizing (41)─(43) and the known stochastic properties, the stepwise-optimal gain $K_{k-\varepsilon}^*$ that minimizes the estimation error $\delta\breve{X}_{k-\varepsilon}$ can be derived:

$$K_{k-\varepsilon}^* = E\left[\delta\overline{X}_{k-\varepsilon}Z_{k-\varepsilon}^T\right]\left\{E\left[Z_{k-\varepsilon}Z_{k-\varepsilon}^T\right]\right\}^{-1} \tag{46}$$

where

$$E\left[\delta\overline{X}_{k-\varepsilon}Z_{k-\varepsilon}^T\right] = M_{k-\varepsilon}H_k^T$$
$$E\left[Z_{k-\varepsilon}Z_{k-\varepsilon}^T\right] = (H_kU_kH_{k-\varepsilon})M_{k-\varepsilon}(H_kU_kH_{k-\varepsilon})^T + r_\phi(H_kU_k)(H_kU_k)^T + r_\rho I \tag{47}$$

As ε approaches zero, one obtains the following relationships:

$$\lim_{\varepsilon\to 0}U_{k-\varepsilon} = U_k,$$
$$\lim_{\varepsilon\to 0}U_kH_{k-\varepsilon} = I,$$
$$M_k := \lim_{\varepsilon\to 0}M_{k-\varepsilon} = U_k\left\{\begin{matrix}H_{k-1}\hat{P}_{k-1}H_{k-1}^T\\ +r_\Phi\begin{bmatrix}I-H_{k-1}(I-K_{k-1}H_{k-1})U_{k-1}\\ -U_{k-1}^T(I-K_{k-1}H_{k-1})^T H_{k-1}^T\end{bmatrix}\end{matrix}\right\}U_k^T,$$
$$K_k := \lim_{\varepsilon\to 0}K_{k-\varepsilon} = M_kH_k^T\begin{bmatrix}H_kM_kH_k^T + r_\rho I\\ +r_\phi H_k(H_k^TH_k)^{-1}H_k^T\end{bmatrix}^{-1}. \tag{48}$$

Utilizing $\overline{P}_k$ shown in (17), M_k and K_k in (50) can also be written as:

$$M_k = \overline{P}_k - r_\Phi U_kU_k^T = \overline{P}_k - r_\Phi(H_k^TH_k)^{-1}$$
$$K_k = \left[\overline{P}_k - r_\Phi(H_k^TH_k)^{-1}\right]H_k^T\left[H_k\overline{P}_kH_k^T + r_\rho I\right]^{-1} \tag{49}$$

As shown in (49), similar to the RD Hatch gain $\beta_{j,k}$ in (38), the derived PD Hatch gain K_k also appears slightly skewed by $r_\phi(H_k^TH_k)^{-1}$ as compared to the Kalman-type gain in (19)─(21).

The derived PD Hatch filter is summarized in Table 1, where a selection matrix Γ_k is used to consider cycle slips and abrupt satellite inclusions and outages. The selection matrix Γ_k consists of 0's and 1's where 1 denotes the measurement that is valid at both the k and $(k-1)$-th step, simultaneously. Thus, the selection matrix Γ_k maps from the full-dimensional measurement vector Ω_k and Z_k that considers all the channels to the reduced measurement vector Y_k^*. By the utilization of the selection matrix Γ_k and single differenced measurements, the exclusion of the multipath or cycle slip affected channel is operationally easy as shown in Fig. 4 compared with the existing position-domain kinematic carrier-smoothed-code methods utilizing double differenced measurements [5], [20].

The following Theorem 2 states that the PD Hatch filter, like the RD Hatch filter, is a generator of white residual sequence. It

means that the PD Hatch filter extracts all the useful information from the pseudorange and incremental carrier phase measurements.

Theorem 2: *White residual generation by PD Hatch filter*

If the noise terms of corrected measurements satisfy (1), the PD Hatch filter represented by (16)− (18) and (51) generates a white residual sequence.

□

IV. Experiment

To evaluate the performance characteristics of the PD Hatch filter, an experiment was performed. For the experiment, two dual-frequency GPS receivers are utilized. One receiver is installed at an exactly known position as a reference and the other is mounted on a test vehicle as a rover. For the experiment, the vehicle was run around a semi-urban area. During the run, all the raw measurements of the reference and rover are logged in the Receiver Independent Exchange Format (RINEX) format. To extract a "truth" trajectory, commercial processing software for Carrier-phase Differential GPS (CDGPS) was utilized. Since the truth trajectory is based on the resolved integer ambiguity in the differenced carrier phase measurements, its typical accuracy is in the order of cm.

For performance comparison, the logged RINEX measurements are utilized as an input to the RD Hatch filter, the PD Kalman-type filter, and the PD Hatch filter in the simulated real-time mode. To highlight the effects of carrier phase noise, wide-lane combination of carrier phase measurements are utilized. To consider the noise amplification by *single-differencing* and wide-lane measurements, the variances of code and carrier noises were set as 1.5 m and 0.09 m, respectively. Before the processing by the candidate filters, the measurements are selected or screened by a channel selection matrix and multiple channelwise fault detectors as shown in Fig. 4. As detailed in [6], the fault detection and isolation scheme is independent of the position estimates generated by the candidate filters. Thus, the same set of measurements is utilized as the input to the candidate filters.

Fig. 5 and Fig. 6 depict the experimental trajectory during the total 2100 seconds in more detail. The test vehicle was run on a horizontal rectangle twice as shown in Fig. 5. In Fig. 5, the left plot shows the overall configuration of the horizontal trajectory and the right plot shows a magnified view of the uppermost spot. In Fig. 6, the gray line with circles corresponds to the CDGPS truth trajectory. As shown by the CDGPS trajectory, the test vehicle spends most of its time at a fixed height and deviates from it twice. Each deviation corresponds to each turning over the rectangle shown in the left plot of Fig. 5. It needs to be noted that the number of visible satellites changes a lot during each turning as shown by the gray line with star symbols in Fig. 6.

Fig. 7 shows the error distance produced by each filter. To compute each error distance, the following equation is utilized.

$$d_k = \left\| \hat{X}_k - X_k^{CDGPS} \right\| \tag{50}$$

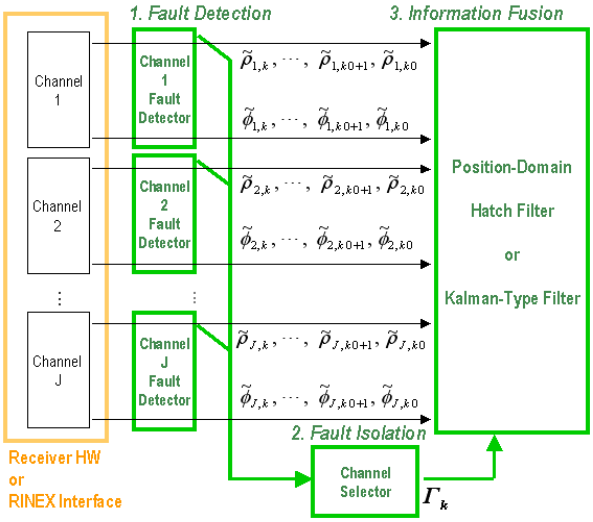

Fig. 4. Implementation architecture for position-domain filters utilizing channel selection matrix

where X_k^{CDGPS} indicates the position estimate provided by the CDGPS. In Fig. 7, the dotted gray line with star symbols corresponds to the RD Hatch filter, the solid gray line corresponds to the PD Kalman-type filter, and the solid black line corresponds to the PD Hatch filter.

In the beginning before approximately 180 seconds, all the filters shows similar trend. During the movement of the vehicle from 180 to 600 seconds approximately, however, it can be seen that the error distance of the RD Hatch filter changes a lot. This result is caused by the frequent changes in visible satellites as shown in Fig. 6.

Between 600 and 1500 seconds during which the vehicle doesn't move, the steady state error characteristics of each filter can be compared. As a whole, it can be seen that the fluctuation between the maximum and minimum values of the error distances becomes smaller in the order of the RD Hatch filter, the PD Kalman-type filter, and the PD Hatch filter. In other words, the PD Hatch filter shows best characteristics in terms of precision. Between the 1700 and 1800 seconds and between the 1900 and 2100 seconds, it can be clearly seen that the maximum error distance reduces in the order of the RD Hatch, the PD Kalman-type filter, and the PD Hatch filter. This means that the PD Hatch filter shows best accuracy .

V. Conclusion

Motivated both by the accuracy benefit of the Hatch gain compared to the Kalman-type gain and the advantage of position-domain filtering compared to range-domain filtering, this paper proposed an alternative carrier-smoothed-code filter for differential kinematic positioning. It was shown that the Hatch gain generates a white residual sequence and the position-domain Hatch filter is more attractive than the range-domain Hatch filter if changes in the visible satellite constellation occur. An experiment result demonstrated that the proposed position-domain Hatch filter attractive in real-time kinematic positioning.

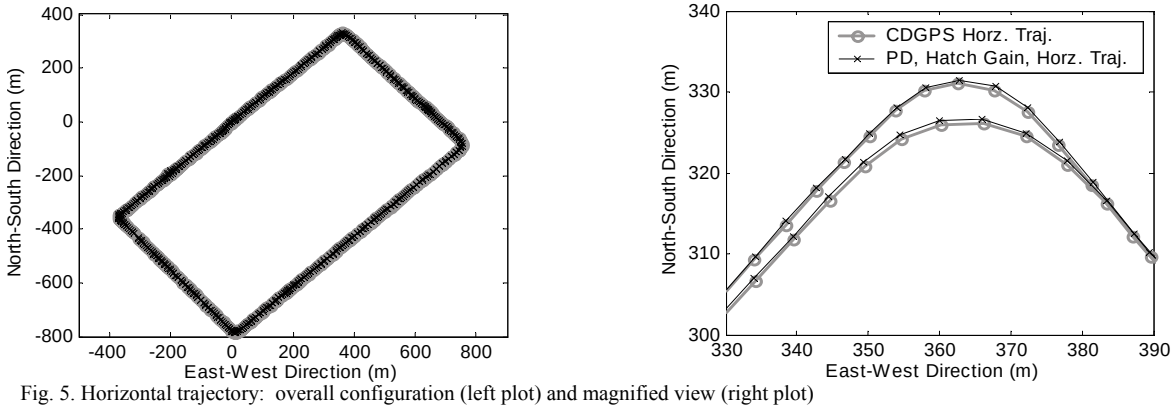

Fig. 5. Horizontal trajectory: overall configuration (left plot) and magnified view (right plot)

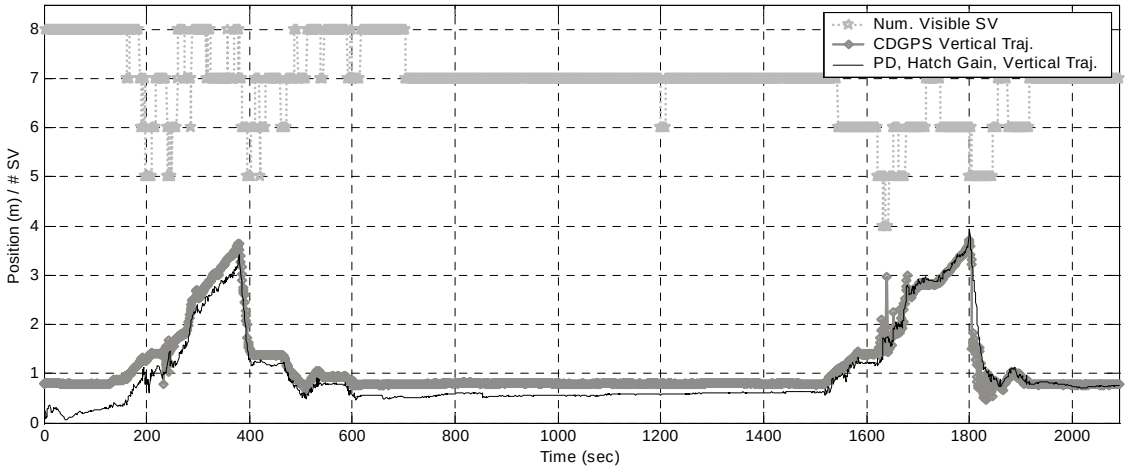

Fig. 6. Vertical trajectory configuration and number of visible satellites

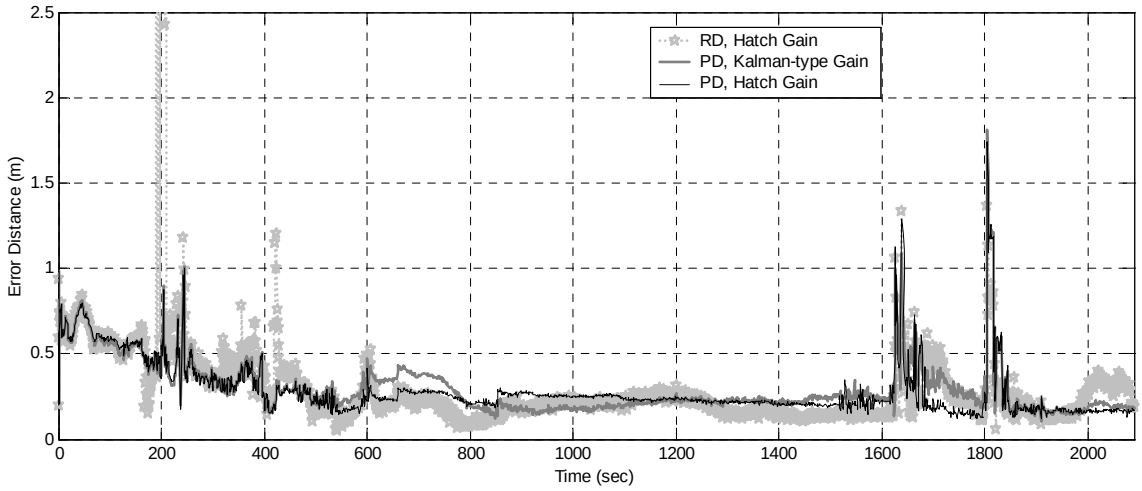

Fig. 7. Comparison of error distance: range-domain Hatch filter, position-domain Kalman-type filter, and position-domain Hatch filter

APPENDIX

A. Proof of **Theorem 1**

Let's denote the $\vartheta_{j,k}$ and $\vartheta_{j,k-1}$ as the measurement residuals of the j-th satellite's channel at the k-th and $(k-1)$-th epochs, respectively:

$$\begin{aligned}\vartheta_{j,k} &= \bar{v}_{j,k} - v_{j,k} \\ \vartheta_{j,k-1} &= \bar{v}_{j,k-1} - v_{j,k-1}\end{aligned} \tag{A1}$$

where the *a priori* range estimation error $\bar{v}_{j,k}$ satisfies:

$$\bar{v}_{j,k} = (1-\beta_{j,k-1})\bar{v}_{j,k-1} + \beta_{j,k-1}v_{j,k-1} + n_{j,k} - n_{j,k-1} \tag{A2}$$

by (25) and (26). Utilizing the correlation between $\bar{v}_{j,k-1}$ and $n_{j,k-1}$ shown in (A2), it can be verified that:

$$E[\vartheta_{j,k}\vartheta_{j,k-1}] = (1-\beta_{j,k-1})\bar{R}_{j,k} - r_\phi - \beta_{j,k-1}r_\rho = 0 \tag{A3}$$

whenever the gain $\beta_{j,k}$ satisfies (23a).

Though not depicted, two measurement residuals more than one epoch apart can also be shown to have zero correlation if the gain $\beta_{j,k}$ satisfies (30). As a result, it can be concluded that the RD Hatch filter is a white residual generator. □

B. Proof of **Theorem 2**

At first, assume that two measurement residuals are separated by one epoch. The measurement residual Z_k is decomposed as follows (utilizing (7) and (17)):

$$\begin{aligned}Z_k &= H_k\delta\bar{X}_k + v_k \\ &= H_kU_k(I - H_{k-1}K_{k-1})Z_{k-1} \\ &\quad + (v_k - H_kU_kv_{k-1}) - H_kU_k(n_k - n_{k-1})\end{aligned} \tag{B1}$$

Based on the correlations between Z_{k-1}, v_{k-1}, and n_{k-1}, it can be shown that:

$$E\left[Z_kZ_{k-1}^T\right] = H_kU_k\left[(I - H_{k-1}K_{k-1})\Sigma_{k-1} - r_\rho I - r_\phi U_{k-1}^T H_{k-1}^T\right] \tag{B2}$$

where

$$\Sigma_{k-1} := H_{k-1}\bar{P}_{k-1}H_{k-1}^T + r_\rho I\,. \tag{B3}$$

For Z_k and Z_{k-1} to be uncorrelated, the following condition should be satisfied since the matrix H_kU_k is, in general, not a zero vector and is time-varying:

$$(I - H_{k-1}K_{k-1})\Sigma_{k-1} - r_\rho I - r_\phi U_{k-1}^T H_{k-1}^T = O \tag{B4}$$

Utilizing (49) for the K_{k-1} shown in (B4), it can be verified that the condition in (B4) is satisfied.

The two measurement residuals separated by more than one epoch can also be shown to be uncorrelated if (B4) is satisfied for every epoch. Thus, the proposed PD Hatch filter generates a white measurement residual sequence. □

ACKNOWLEDGMENT

This work has been supported by Korea Science and Engineering Foundation (KOSEF) and the Satellite Navigation and Positioning group at The University of New South Wales.

REFERENCES

[1] R.R. Hatch, "The synergism of GPS code and carrier measurements," *Proceedings of the Third International Geodetic Symposium on Satellite Doppler Positioning,* New Mexico, **II**, pp. 1213-1232, 1982

[2] P.Y.C. Hwang and R.G. Brown, "GPS navigation: combining pseudorange with continuous carrier phase using a Kalman filter," *Navigation: Journal of The Institute of Navigation*, vol. 37, no. 2, pp. 181-196, 1990

[3] S.B. Bisnath and R.B. Langley, "Precise, efficient GPS-based geometric tracking of low earth orbiters," *Proceedings of the Institute of Navigation Annual Meeting*, Cambridge, Massachusetts, pp. 751-760, 1999

[4] F. van Graas, and S.W. Lee, "High-accuracy differential positioning for satellite-based systems without using code-phase measurements," *Navigation: Journal of The Institute of Navigation*, vol. 42, no. 4, pp. 605-618, 1995

[5] H. Leppakoski, J. Syrjarinne, and J. Takala, "Complementary Kalman filter for smoothing GPS position with GPS velocity," Proceedings of. ION GPS/GNSS 2003, 9-12 Sept. 2003, Portland, pp. 1201-1210.

[6] H. K. Lee, J. G. Lee, and G. I. Jee, "An efficient GPS receiver algorithm for channelwise multipath detection and real-time positioning," *Proceedings of the Institute of Navigation 2002 National Technical Meeting*, San Diego, CA, pp. 265-276, 2002

[7] H. K. Lee, C. Rizos, and G. I. Jee, "Design of kinematic DGPS filters with consistent error covariance information", *IEE Proceedings - Radar, Sonar and Navigation*, Vol. 151, No. 6, pp.382-388, 2004

[8] H. K. Lee, C. Rizos, and G. I. Jee, "Position domain filtering and range domain filtering for carrier-smoothed-code DGNSS: an analytical comparison", *IEE Proceedings - Radar, Sonar and Navigation*, Vol. 152, No. 4, pp.271-276, 2005

[9] B.Parkinson and P. Axelad, *Global Positioning System: Theory and Applications*. American Institute of Aeronautics and Astronautics, 1996

[10] J.A. Farrell and M. Bath, *The Global Positioning System And Inertial Navigation*. Mcgraw-Hill, 1998

[11] R.G. Brown and P.Y.C. Hwang, *Introduction to Random Signals and Applied Kalman Filtering.* John Wiley & Sons, 1997

[12] P.Y.C. Hwang, G. A. McGraw, and J. R. Bader, "Enhanced differential GPS carrier-smoothed code processing using dual-frequency measurements," *Navigation: Journal of The Institute of Navigation,* vol. 46, no. 2, pp. 127-137, 1999

[13] P. Mistra, and P. Enge, *Global Positioning System Signals, Measurements, and Performance*. Ganga-Jamuna Press, 2001

[14] R. D. J. van Nee, "The multipath estimating delay lock loop: approaching theoretical accuracy limits," *Proceedings of Position Location and Navigation Symposium*, Las Vegas, Nevada, pp. 246 –251, 1994

[15] M. S. Braasch, "GPS multipath model validation," *Proceedings of Position Location and Navigation Symposium*, Atlanta, GA, pp. 672-678, 1996

[16] D. J. Jwo, "Optimization and sensitivity analysis of GPS receiver tracking loops in dynamic environments," *IEE Proceedings-Radar, Sonar and Navigation,* vol. 148, no. 4, pp. 241-250, 2001

[17] P. Axelrad, C. J. Comp, and P.F. Macdoran, "SNR-based multipath error correction for GPS differential phase," *IEEE Tr. on Aerospace and Electronic Systems*, vol. 32, no. 2, pp. 650-660, 1996

[18] C. D. Kee and B. Parkinson, "Calibration of multipath errors on GPS pseudorange measurements," *Proceedings of the 7th International Technical Meeting of the Satellite Division of The Institute of Navigation*, Salt Lake City, Utah, pp. 352-362, 1994

[19] J. K. Ray, M. E. Cannon, and P. Fenton, "GPS code and carrier multipath mitigation using a multi antenna system," *IEEE Tr. on Aerospace and Electronic Systems*, vol. 37, no. 1, pp. 183-195, 2001

[20] H. K. Lee, J. G. Lee, and G. I. Jee, "GPS multipath detection based on successive-time double-differences", *IEEE Signal Processing Letters*, Vol. 11, No. 3, pp. 316-319, 2004.

[21] N. A. Carlson, "Federated square root filter for decentralized parallel processes," *IEEE Transactions on Aerospace and Electronic Systems*, vol. 26, no. 3, pp. 517-525, 1990

[22] T. Kailath, A. H. Sayed, and B. Hassibi, *Linear Estimation,* Prentice Hall, 2000

TABLE 1
POSITION-DOMAIN HATCH FILTER

Initialization:

$$H^*_{k0} = \Gamma_{k0} H_{k0}$$

$$\hat{X}_{k0} = E[X_{k0} \mid \Gamma_{k0}\tilde{\rho}_{k0}], \quad \hat{P}_{k0} = r_\rho[(H^*_{k0})^T H^*_{k0}]^{-1}$$

Time-Propagation:

$$H^*_{k+1} = \Gamma_{k+1} H_{k+1}, \quad H^p_k = \Gamma_{k+1} H_k, \quad \Omega^*_{k+1} = \Gamma_{k+1}\Omega_{k+1}$$

$$U^*_{k+1} = [(H^*_{k+1})^T H^*_{k+1}]^{-1}(H^*_{k+1})^T$$

$$\overline{X}_{k+1} = \hat{X}_k + U^*_{k+1}\Omega^*_{k+1}$$

$$\overline{P}_{k+1} = U^*_{k+1}\left\{H^p_k \hat{P}_k (H^p_k)^T + r_\phi \begin{bmatrix} 2I - H^p_k\left(I - K^*_k H^*_k\right)U^*_k\Gamma_k\Gamma^T_{k+1} \\ -\Gamma_{k+1}\Gamma^T_k (U^*_k)^T\left(I - K^*_k H^*_k\right)^T (H^p_k)^T \end{bmatrix}\right\}(U^*_{k+1})^T$$

Measurement Update:

$$K^*_k = \left\{\overline{P}_k - r_\phi\left[(H^*_k)^T H^*_k\right]^{-1}\right\}(H^*_k)^T\left[H^*_k \overline{P}_k (H^*_k)^T + r_\rho I\right]^{-1}$$

$$Z^*_k = \Gamma_k Z_k$$

$$\hat{X}^*_k = \overline{X}^*_k - K^*_k Z^*_k,$$

$$\hat{P}^*_k = \left(I - K^*_k H^*_k\right)\overline{P}^s_k\left(I - K^*_k H^*_k\right)^T + r_\rho K^*_k (K^*_k)^T$$